Human Molecular Genetics, 2010, Vol. 19, No. 18 **3557–3565**
doi:10.1093/hmg/ddq271
Advance Access published on July 16, 2010

Cadherin-23, myosin VIIa and harmonin, encoded by Usher syndrome type I genes, form a ternary complex and interact with membrane phospholipids

Amel Bahloul[1,2,3], Vincent Michel[1,2,3], Jean-Pierre Hardelin[1,2,3], Sylvie Nouaille[1,2,3], Sylviane Hoos[4,5], Anne Houdusse[6], Patrick England[4,5] and Christine Petit[1,2,3,7,*]

[1]Département de Neuroscience, Unité de Génétique et Physiologie de l'Audition, Institut Pasteur, 25 rue du Dr Roux, 75724 Paris cedex 15, France, [2]Inserm UMRS 587, Paris, France, [3]Université Pierre-et-Marie Curie, Paris, France, [4]Plate-Forme de Biophysique des Macromolécules et de leurs Interactions, Institut Pasteur, 75015 Paris, France, [5]CNRS URA 2185, Paris, France, [6]Institut Curie CNRS, UMR144, 75248 Paris cedex 05, France and [7]Collège de France, 75005 Paris, France

Received May 27, 2010; Revised and Accepted June 26, 2010

Cadherin-23 is a component of early transient lateral links of the auditory sensory cells' hair bundle, the mechanoreceptive structure to sound. This protein also makes up the upper part of the tip links that control gating of the mechanoelectrical transduction channels. We addressed the issue of the molecular complex that anchors these links to the hair bundle F-actin core. By using surface plasmon resonance assays, we show that the cytoplasmic regions of the two cadherin-23 isoforms that do or do not contain the exon68-encoded peptide directly interact with harmonin, a submembrane PDZ (post-synaptic density, disc large, zonula occludens) domain-containing protein, with unusually high affinity. This interaction involves the harmonin Nter-PDZ1 supramodule, but not the C-terminal PDZ-binding motif of cadherin-23. We establish that cadherin-23 directly binds to the tail of myosin VIIa. Moreover, cadherin-23, harmonin and myosin VIIa can form a ternary complex, which suggests that myosin VIIa applies tension forces on hair bundle links. We also show that the cadherin-23 cytoplasmic region, harmonin and myosin VIIa interact with phospholipids on synthetic liposomes. Harmonin and the cytoplasmic region of cadherin-23, both independently and as a binary complex, can bind specifically to phosphatidylinositol 4,5-bisphosphate ($PI(4,5)P_2$), which may account for the role of this phospholipid in the adaptation of mechanoelectrical transduction in the hair bundle. The distributions of cadherin-23, harmonin, myosin VIIa and $PI(4,5)P_2$ in the growing and mature auditory hair bundles as well as the abnormal locations of harmonin and myosin VIIa in cadherin-23 null mutant mice strongly support the functional relevance of these interactions.

INTRODUCTION

Auditory sensory cells (hair cells) convert acoustic mechanical energy into electrical receptor potential by means of a morphologically and functionally polarized apical structure called the hair bundle. This is a V- or U-shaped ensemble of actin-filled modified microvilli, known as stereocilia, that are arranged into three to four height-ranked rows. The immature hair bundle also contains a genuine cilium, the kinocilium. Transient fibrous lateral links connect early growing stereocilia together and to the kinocilium (1–3). Identification of the genes defective in Usher syndrome type I (USH1), a recessive disease characterized by congenital profound deafness, vestibular dysfunction and delayed onset retinopathy leading to blindness, has led to the characterization of two major components of these links, namely cadherin-23 and most likely protocadherin-15 (4,5) that are encoded by *USH1D* (6,7) and *USH1F* (8,9), respectively. The three other USH1 genes

*To whom correspondence should be addressed. Tel: +33 145688890; Fax: +33 140613442; Email: christine.petit@pasteur.fr

known to date encode the scaffolding submembrane protein harmonin (USH1C) (10,11), the actin-based motor protein myosin VIIa (USH1B) (12) and the putative scaffolding protein sans (USH1G) (13). The early disorganization of the growing hair bundle that is common to mutant mice defective for any of the *Ush1* genes (14), the similar, apical end distributions of cadherin-23, protocadherin-15, harmonin and myosin VIIa in the growing hair bundle and the interdependent locations of some of these proteins (14–16), along with evidence for direct physical interactions *in vitro* (13,15–19), together suggest that these proteins may form molecular complexes associated with the transient lateral links. In addition, cadherin-23 and protocadherin-15 make up the upper and lower part of the tip link, respectively (20,21). This single oblique link runs from the tip of each stereocilium to the side of the adjacent stereocilium from the taller row in the mature hair bundle (22). The tip link transmits sound-evoked tension forces to the mechanically gated transduction channel, of as yet unknown molecular composition. Both the connection of the basal part of the tip link to the transduction channel and the anchoring of its upper part to the stereocilia actin filaments that involves the locally restricted harmonin-b isoforms are expected to play essential roles in this process (15,23,24). Here, we studied the as yet poorly characterized cadherin-23-associated molecular complexes that may anchor the transient lateral links and the upper part of the tip link in the stereocilia.

RESULTS AND DISCUSSION

Cadherin-23 binds to harmonin with a high affinity

Based on the analysis of *Ush1c* transcripts in the mouse inner ear, three classes of harmonin isoforms (a, b and c) are predicted (25) (Fig. 1). All contain an N-terminal domain (Nter) followed by two PDZ (post-synaptic density, disc large, zonula occludens) domains and a predicted coiled-coil domain. Isoforms a and b also contain a third PDZ domain located at their C-terminal end preceded, in isoforms b only, by an additional coiled-coil domain and a proline–serine–threonine-rich sequence. It is still unknown whether harmonin isoforms a and c are present in the hair bundle. We produced a specific polyclonal antibody (harmonin-H1) against Nter (see Materials and Methods). From the comparison of the immunostaining patterns obtained in mice with this anti-pan-harmonin and an anti-harmonin-b antibody, we could conclude that harmonin isoforms a/c are present along the stereocilia, forming immunoreactive patches both in growing (P1) and mature (P15) hair bundles (Supplementary Material, Fig. S1). The labeling was more intense in mature hair bundles. Isoforms a/c were detected at the tips of stereocilia from the small and mid rows, suggesting the possible association of these isoforms with the tip-link lower insertion point. They were also detected in the apical region of tallest stereocilia that extends above the tip-link upper insertion point. It has been reported that cadherin-23 binds to the Nter, PDZ1 and PDZ2, but not PDZ3 domains of harmonin *in vitro* (15,17,19). Therefore, cadherin-23 is expected to interact with all harmonin isoforms. In addition, two cadherin-23 isoforms that do or do not contain the exon 68-encoded 35 amino acids insert have been reported (17) (Fig. 1). Based on pull-down assays, the C-terminal consensus PDZ-binding motif (ITEL) of cadherin-23 had previously been reported to be involved in the binding of cadherin-23 to harmonin, and the absence of the exon 68–encoded insert has been proposed to enhance this binding, possibly by unmasking an internal PDZ-binding sequence (17).

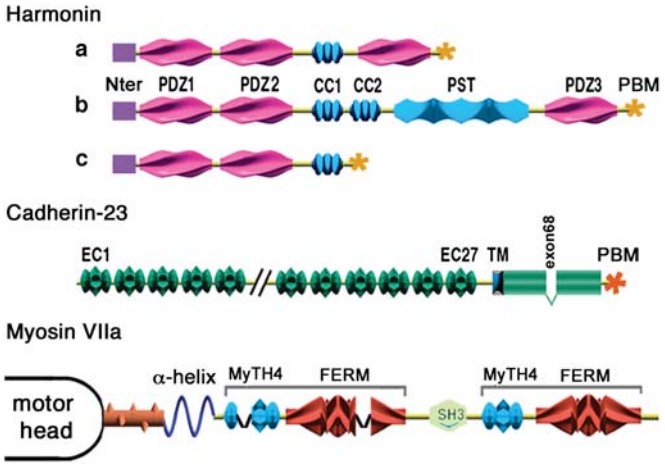

Figure 1. Schematic representation of myosin VIIa, harmonin and cadherin-23 isoforms. Abbreviations: Nter, N-terminal; PDZ, post-synaptic density, disc large, zonula occludens; CC, coiled-coil; PST, proline-, serine-, threonine-rich; PBM, PDZ-binding motif; EC, extracellular; TM, transmembrane; MyTH4, myosin tail homology 4; FERM, band 4.1, ezrin, radixin, moesin; SH3, src homology 3.

To analyze cadherin-23/harmonin interactions, we produced the entire cytoplasmic regions of both cadherin-23 isoforms (CDH23 + exon68 and CDH23Δexon68) and the full-length harmonin-a isoform. We determined the harmonin-a concentration dependence of the steady-state binding signal to either CDH23 + exon68 or CDH23Δexon68 using a surface plasmon resonance (SPR) assay. The equilibrium dissociation constants (K_d) were very similar for both CDH23 isoforms (Table 1), which argues against exon 68 playing a significant role in harmonin binding. Surprisingly, these K_d values (97 ± 14 and 79 ± 11 nM) are much lower than those reported for the interaction of single PDZ domains with their binding partners (26). Because such a high-affinity cadherin-23/harmonin-a interaction could result from the involvement of several harmonin-a domains, we studied the interactions of truncated forms of harmonin-a with CDH23. No binding signal could be detected for either the Nter or the PDZ3 domains alone—proper folding of both truncated proteins was checked by circular dichroism experiments—at the highest concentration used (500 nM), which indicates that the corresponding K_d values are higher than 5 μM. This value is consistent with the previously reported K_d (25 μM) of the complex between Nter and a 20-residue CDH23 peptide (19). In contrast, the affinities of the Nter-PDZ1 fragment for the two CDH23 isoforms were similar to those of the full-length harmonin-a, while those of the Nter-PDZ1-PDZ2 fragment were only 1.5–1.9 times higher (Table 1). We deleted the C-terminal consensus PDZ-binding motif (ITEL) in both CDH23 isoforms and studied the binding of these ΔITEL fragments to harmonin-a, Nter-PDZ1-PDZ2 and Nter-PDZ1. The K_d

Table 1. Dissociation equilibrium constants (K_d) of the interaction between harmonin-a and cadherin-23 constructs

	CDH23 + exon68	CDH23Δexon68	CDH23 + exon68ΔITEL	CDH23Δexon68ΔITEL
Full-length harmonin a	97 ± 14 nM	79 ± 11 nM	127 ± 12 nM	48 ± 6 nM
Nter-PDZ1-PDZ2	64 ± 6 nM	42 ± 11 nM	66 ± 13 nM	30 ± 6 nM
Nter-PDZ1	94 ± 8 nM	79 ± 10 nM	106 ± 5 nM	58 ± 9 nM
Nter	>5000 nM	>5000 nM	>5000 nM	>5000 nM
PDZ3	>5000 nM	>5000 nM	>5000 nM	>5000 nM

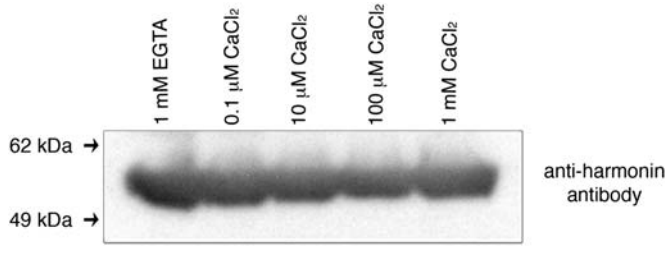

Figure 2. Harmonin-a interacts with CDH23 + exon68 independently of the Ca^{2+} concentration. *In vitro* binding assay. The GST-CDH23 + exon68 fusion protein was immobilized on glutathione–Sepharose. The presence of a harmonin-a/CDH23 + exon68 complex was revealed by western blot analysis, using an anti-harmonin antibody. The positions of the 62 and 49 kDa molecular mass markers are indicated on the left. Note that the complex formed at all Ca^{2+} concentrations tested (between 1 mM and 0.1 μM $CaCl_2$), and in the virtual absence of Ca^{2+} (1 mM EGTA).

values for the ΔITEL fragments were similar to those for the entire CDH23 isoforms, showing that the ITEL motif of CDH23 does not play an important role in the strengthening of the cadherin-23/harmonin-a complex (Table 1). This result, combined with the unusually low K_d values we measured, suggests that the binding mechanism between harmonin-a and cadherin-23 is non-canonical. Accordingly, the defective mechanoelectrical transduction resulting from the missense mutation that has been introduced in the PDZ2 domain of murine harmonin (*harmonin-PDZ2*^{AAA} allele) and predicted to disrupt the binding to the ITEL motif of cadherin-23 (23) is in fact more likely to be explained by the abnormal interaction between harmonin and other proteins containing a consensus PDZ-binding motif, which may include protocadherin-15.

Finally, considering the periodic changes in the hair bundle intracellular Ca^{2+} concentration that come with auditory mechanoelectrical transduction (27), we explored the role of Ca^{2+} ions in the cadherin-23/harmonin-a interaction using a pull-down assay (Fig. 2). An interaction between CDH23 + exon68 and harmonin-a was detected both at high and low Ca^{2+} concentrations and in the virtual absence of Ca^{2+} (1 mM EGTA).

Our results go beyond the previously proposed multidentate binding mechanism between CDH23 and harmonin, involving both its Nter and PDZ2 domains (19). In contrast to these two low-affinity interactions ($K_d = 25$ and 10 μM, respectively), the 100-fold higher affinity we report for the interaction between CDH23 and the Nter-PDZ1 fragment of harmonin-a suggests a so far unsuspected stability of the cadherin-23/harmonin complex. It has been shown that the Nter-PDZ1 harmonin fragment forms a structural supramodule, in which the Nter and PDZ1 domains are tethered together (28). This supramodular structure might be responsible for the high-affinity binding of harmonin to CDH23. Furthermore, the 1D NMR spectra we performed on the Nter-PDZ1-PDZ2 fragment showed that it is well folded and that it does not contain a flexible region (see Supplementary Material, Fig. S2), a result confirmed by the absence of cross peaks in a 2D total correlated spectroscopy experiment (data not shown). This suggests that the PDZ1 and PDZ2 domains may also be held together by inter-PDZ domain interactions, therefore extending the supramodular organization of harmonin isoforms.

Cadherin-23 interacts directly with the myosin VIIa tail

We have previously shown by pull-down experiments that the PDZ1 domain of harmonin binds to the myosin VIIa tail (15). Interaction between the myosin VIIa tail and harmonin-a or its Nter-PDZ1 fragment was investigated by SPR. A K_d close to 1 μM was found in both cases (Fig. 3A and data not shown).

Both myosin-1c and myosin VIIa have been implicated in the adaptation of mechanoelectrical transduction upon sustained deflection of the hair bundle (29,30). Accordingly, myosin-1c has been reported to co-immunoprecipitate with cadherin-23 in transfected cells (30). We therefore sought a possible myosin VIIa–cadherin23 interaction and indeed detected a direct interaction of CDH23 with the myosin VIIa tail by SPR ($K_d = 1.5$ μM; Fig. 3A). The micromolar affinities of the complexes of the myosin VIIa tail with either harmonin-a or CDH23 are about 10 times lower than the affinity of the CDH23/harmonin-a complex (see above). Thus, myosin VIIa interacts *in vitro* with all the known USH1 proteins, i.e. cadherin-23, harmonin, sans and the CD1 isoform of protocadherin-15 (15,16,18), as does harmonin (18).

Cadherin-23, harmonin and myosin VIIa can form a ternary complex

We then addressed the possibility that cadherin-23, harmonin and myosin VIIa form a ternary complex. The myosin VIIa tail was flowed in an SPR biosensor over either immobilized harmonin-a alone or a pre-formed CDH23/harmonin-a complex. The binary complex bound significantly more myosin VIIa tail than harmonin-a alone (Fig. 3B), indicating that the myosin VIIa tail can interact simultaneously with CDH23 and harmonin-a, forming a ternary complex *in vitro*. The myosin VIIa-binding sites on CDH23 and harmonin-a are thus likely to be distinct from those involved in the formation of the CDH23/harmonin-a binary complex.

To assess the physiological relevance of the ternary complex, we studied the distributions of harmonin isoforms

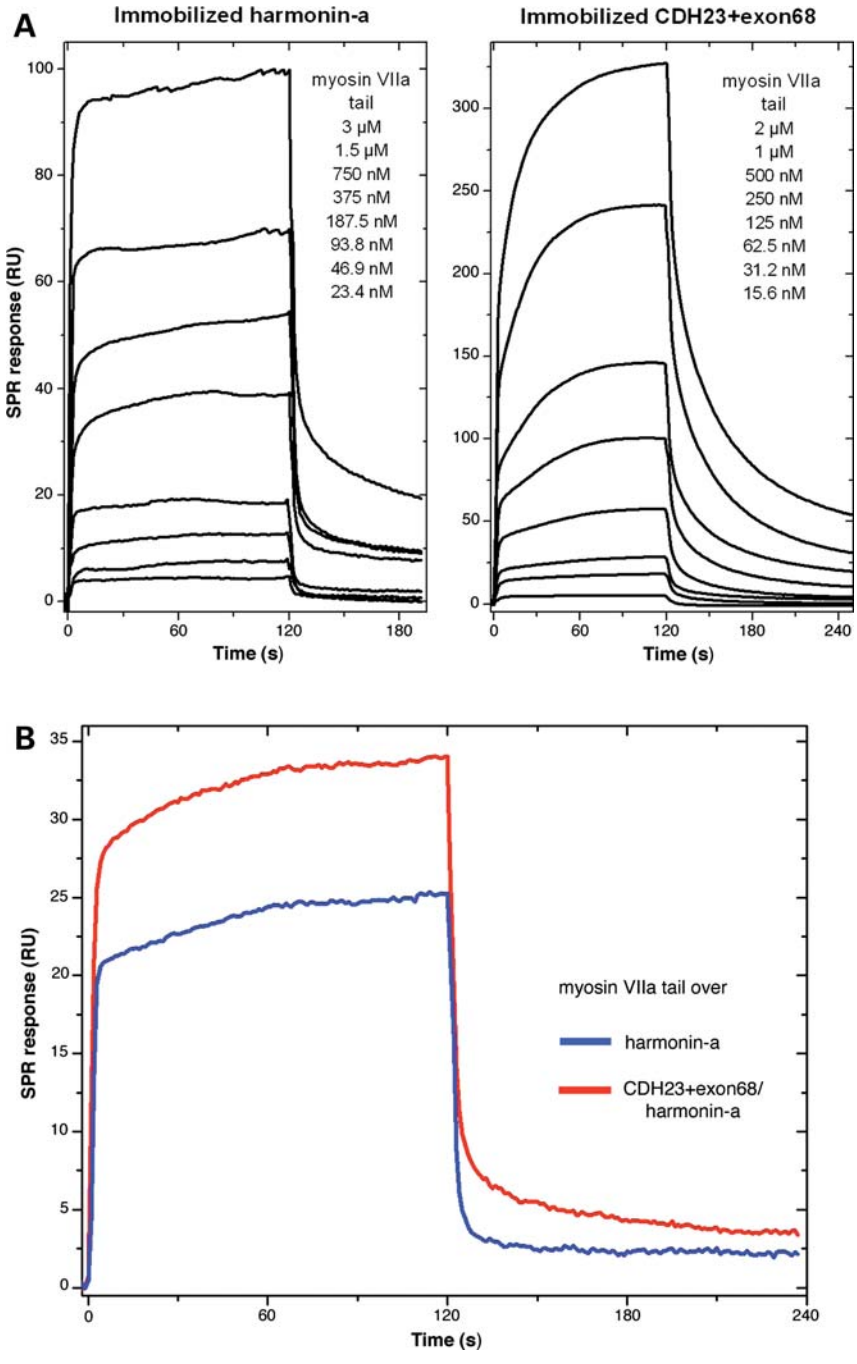

Figure 3. Interactions between cadherin-23, harmonin-a and myosin VIIa. (**A**) Myosin VIIa binds to harmonin-a and cadherin-23. The interaction of the myosin VIIa tail with immobilized full-length harmonin-a (left) or CDH23 + exon68 (right) was monitored by SPR. Different concentrations of the myosin VIIa tail (23.4–3000 or 15.6–2000 nM) were injected in a randomized order. K_d and their respective standard deviations were determined. RU, resonance unit. (**B**) Harmonin-a and cadherin-23 can recruit myosin VIIa simultaneously. The myosin VIIa tail (125 nM) was injected over immobilized harmonin-a, which had been pre-equilibrated or not with CDH23 + exon68 (125 nM). The SPR response corresponding to the binding of myosin VIIa tail to the harmonin-a/CDH23 + exon68 complex (red curve) was higher than that to harmonin alone (blue curve).

and myosin VIIa in the growing hair bundles from cadherin-23-null mutant mice at P1. In these mice, harmonin could not be detected anymore at the hair bundle apex, and myosin VIIa, instead of being restricted to the hair bundle apex, was now distributed along the stereocilia, with a markedly decreased immunostaining (Fig. 4). We conclude that the apical location of harmonin and myosin VIIa in the growing hair bundle critically depends on the presence of cadherin-23. Therefore, a ternary molecular complex involving cadherin-23, harmonin and myosin VIIa is likely to exist also *in vivo*. In this complex, myosin VIIa may exert tension forces on the transient lateral links of the growing

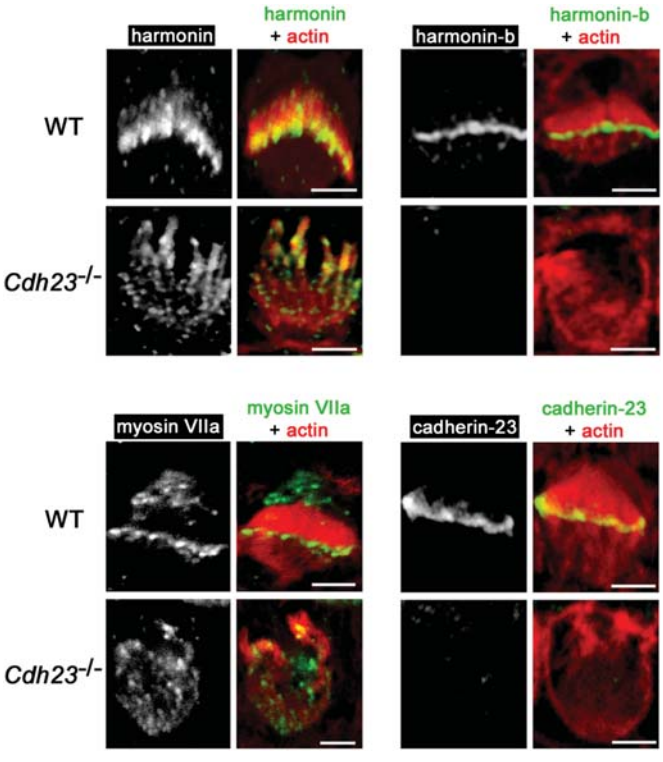

Figure 4. Abnormal distributions of myosin VIIa and harmonin in the hair bundles from early post-natal (P1) cadherin-23-null mutant mice. The distributions of harmonin isoforms, myosin VIIa and cadherin-23 are shown in the hair bundle of outer hair cells from wild-type (WT) and cadherin-23-null (*Cdh23*$^{-/-}$) mice. Actin filaments have been stained using TRITC-conjugated phalloidin (red). Note the absence of any harmonin-b and cadherin-23 immunostainings and the abnormal locations of myosin VIIa and other harmonin isoforms in the *Cdh23*$^{-/-}$ hair bundles. Scale bars: 2 μm.

hair bundle, thereby contributing to its cohesion. Myosin VIIa may also contribute to the tip-link tension that is thought to control the gating of mechanoelectrical transduction channels in the mature hair bundle. Indeed, the high duty ratio of vertebrate myosin VII motors combined with their low ATPase activity qualify these myosins to exert local tension forces (31–33).

Cadherin-23, harmonin and myosin VIIa bind to phosphorylated forms of phosphatidylinositol including phosphatidylinositol 4,5-bisphosphate

Given the paramount roles of harmonin, myosin VIIa, cadherin-23 and phosphorylated forms of phosphatidylinositol (PIP) in mechanoelectrical transduction and its adaptation process (24,29,30,34), we asked whether the three proteins could directly interact with membranes containing phosphatidylinositol (PI) lipids. Despite a basal binding to non-phosphorylated PI-containing liposomes, the liposome-binding of CDH23 and, to a lesser degree, that of harmonin-a was largely dependent on the presence of a phosphorylated PI head [4P, 5P, (4,5)P_2], whereas the binding of the myosin VIIa tail was mostly PIP-independent (Fig. 5A). Incidentally, the binding of harmonin to phospholipids is likely to involve its PDZ domains because PDZ domains have been reported to interact with PIP (35). The binding of CDH23 correlated with the proportion of phosphatidylinositol 4,5-bisphosphate [PI(4,5)P_2] in the liposomes to a greater degree than that of harmonin-a and the myosin VIIa tail, thus confirming the binding specificity of CDH23 for PI(4,5)P_2 (Supplementary Material, Fig. S3). Notably, CDH23 tethered to the PI(4,5)P_2 liposomes could still recruit harmonin-a (Fig. 5B), thus suggesting that cadherin-23 contains different binding sites for PI(4,5)P_2 and harmonin-a. To assess the physiological relevance of these results, we co-transfected HeLa cells with expression vectors encoding the eGFP-fused cytoplasmic region of cadherin-23 (eGFP-CDH23) and the myc tag-fused pleckstrin homology domain of phospholipase C (Myc-PH), used as a PI(4,5)P_2 reporter (36). The eGFP-CDH23 and myc-PH proteins entirely co-localized at the plasma membrane in speckled immunostainings. Likewise, an eGFP–harmonin-a construct co-localized with myc-PH at the plasma membrane in co-transfected HeLa cells, but only after treating the cells with hydrogen peroxide (H_2O_2), which increases the PI(4,5)P_2 concentration (37) (Fig. 6).

In mouse auditory hair cells, PI(4,5)P_2 immunoreactivity could be detected along the stereocilia of growing and mature hair bundles (Fig. 7) (30). The presence of PI(4,5)P_2 in the apical region of the growing hair bundles thus argues in favor of the existence of a molecular complex associated with CDH23 at the insertion points of early transient lateral links, which also involves harmonin, myosin VIIa and plasma membrane PI(4,5)P_2, and would be anchored to the stereocilia actin cytoskeleton through myosin VIIa and harmonin-b isoforms that can bind to F-actin (15). This complex is required for the structural integrity of growing hair bundles, as indicated by their early fragmentation in mutant mice defective for myosin VIIa, harmonin or cadherin-23 (14). In addition, we and others have shown that in mature hair bundles, these proteins are present in the region of the tip-link upper insertion point: cadherin-23 and harmonin-b have locally restricted distributions (14,23,24), while myosin VIIa is detected all along the stereocilia (V.M., unpublished data). Moreover, myosin VIIa, harmonin-b and PI(4,5)P_2 have all been implicated in the adaptation process of mechanoelectrical transduction that re-sets the sensitivity of the transduction channels while the mechanical stimulation of the hair bundle is maintained (24,29,34). We suggest that a molecular complex similar to that observed in the apical region of growing stereocilia also exists at the tip-link upper insertion point in mature stereocilia. The stability of the interaction between harmonin and cadherin-23 whatever the Ca^{2+} concentration (see Supplementary Material, Fig. S2) indicates that this particular interaction is not a target of the Ca^{2+} modulation of adaptation (27). Still, the binding of the cadherin-23/harmonin complex to PI(4,5)P_2 may account for the reported PI(4,5)P_2 dependence of adaptation. In the adaptation process driven by a sustained deflection of the hair bundle towards the tallest stereocilia, harmonin-b limits the reclosure of the transduction channels, likely by preventing the full relaxation of the tip-link tension (24). Incidentally, the direct binding of myosin VIIa to cadherin-23 may explain the persisting anchoring of the tip link to the stereocilia actin filaments in the absence of

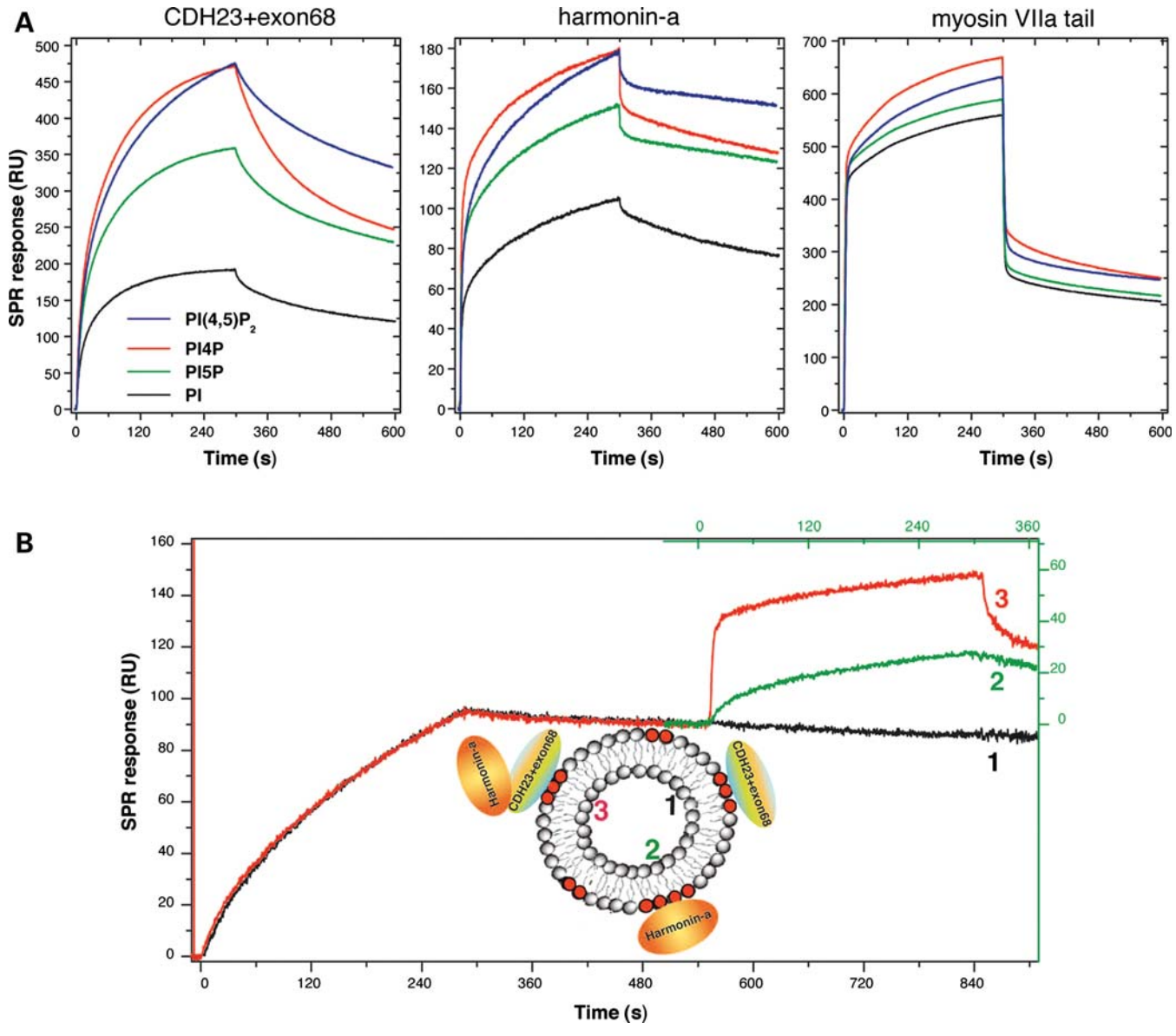

Figure 5. Interactions of cadherin-23, harmonin and myosin VIIa with phospholipids. (**A**) Binding to non-phosphorylated and phosphorylated forms of PI. Real-time SPR profiles showing the interaction of full-length harmonin-a, myosin VIIa tail or CDH23 + exon68 (1.25 μM each) with immobilized liposomes containing 20% of PI, PI4P, PI5P or $PI(4,5)P_2$. The binding of CDH23 + exon68 and harmonin-a depended strongly on the phosphorylation of the PI lipids, unlike that of myosin VIIa. (**B**) $PI(4,5)P_2$-tethered cadherin-23 is able to bind to harmonin-a. Real-time SPR profiles showing the interaction with immobilized 20% $PI(4,5)P_2$-containing liposomes of the following proteins (250 nM): CDH23 + exon68 alone (1, black curve and scale), full-length harmonin-a alone (2, green curve and scale) or CDH23 + exon68 followed by harmonin-a (3, red curve and scale).

harmonin-b (24). Finally, we propose that the cadherin-23/harmonin complex, by virtue of its direct binding to $PI(4,5)P_2$, contributes to the plasma membrane curvature that is observed at the tip-link upper insertion point.

MATERIALS AND METHODS

Preparation of proteins

The following coding sequences were amplified and cloned into a pGST//1 vector (derived from pGEX-4T-1; Amersham) for expression in *Escherichia coli* prokaryotic cells or in pFast Bac (GE Healthcare) for expression in SF9 insect cells (baculovirus system): full-length harmonin-a (accession no. AF228924) and its Nter (residues 1–79), Nter-PDZ1 (1–203), Nter-PDZ1-PDZ2 (1–299), PDZ3 (434–545) truncated fragments; the cytoplasmic region of cadherin-23 either including the sequence encoded by exon68 (CDH23 + exon68, residues 847–1114 and 847–1110; accession no. AY563163.1) or lacking this sequence (CDH23Δexon68, residues 847–1079 and 847–1075; accession no. AY563164.1). Proteins were produced in BL21(DE3)codonPlus-RP *E. coli* cells. The glutathione *S*-transferase (GST)-tagged proteins were purified using a glutathione Sepharose 4B column, fol-

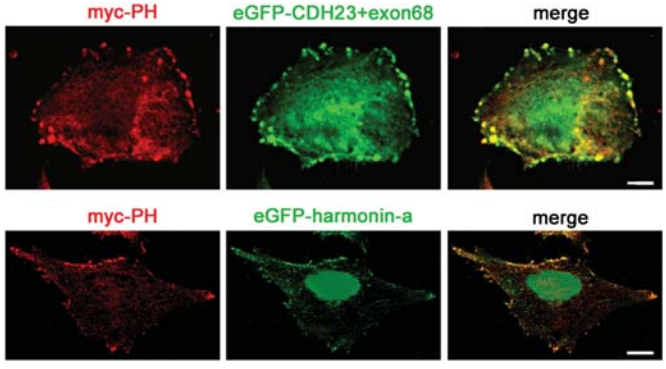

Figure 6. Colocalization of PI(4,5)P_2 with either cadherin-23 or harmonin-a in transfected HeLa cells. Upper panel: CDH23 + exon68 fused to eGFP (eGFP-CDH23 + exon68) and the myc-tagged PH domain of phospholipase C (myc-PH), used as a PI(4,5)P_2 reporter, co-localized at the plasma membrane. Lower panel: full-length harmonin-a fused to eGFP (eGFP-harmonin-a) and myc-PH co-localized at the plasma membrane after H_2O_2 treatment of the cells. Scale bars: 5 μm.

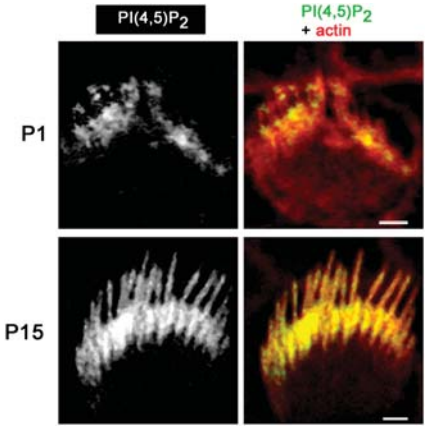

Figure 7. PI(4,5)P_2 immunodetection in growing (P1) and mature (P15) hair bundles from mouse outer hair cells. Scale bars: 1 μm.

lowed by size-exclusion chromatography. For the different harmonin-a constructs, the GST tag was removed using recombinant tobacco etch virus NIa proteinase. The cadherin-23 fragments were eluted from a glutathione Sepharose 4B column with reduced glutathione. The integrity of the different cadherin-23 fragments was verified by mass spectrometry (QSTAR XL QqTOF mass spectrometer; AB-MDS-Sciex, Thornill, Canada). For some SPR experiments, the CDH23 + exon68 fragment was produced in SF9 cells using the baculovirus expression system. The His_6-tagged CDH23 + exon68 fragment was purified using Ni-NTA agarose beads, followed by size-exclusion chromatography. The His_6-tagged tail of myosin VIIa was purified as previously described (15).

Antibodies

The following primary antibodies were used: rabbit polyclonal antibodies against myosin VIIa (15,38), harmonin-b (15) or cadherin-23 (14), mouse monoclonal IgG against Myc (mAb 9E10 from Santa Cruz Biotechnology) and IgM against PI(4,5)P_2 (mAb 2C11 from Molecular Probes, Eugene). For harmonin distribution studies in hair cells, a rabbit antiserum (harmonin-H1; 1:500) was produced against the Nter fragment. Primary antibodies were detected using Alexa488- or Cy3-conjugated secondary antibodies (Molecular Probes). F-actin was visualized with TRITC-conjugated phalloidin (Sigma).

In vitro binding experiments

To explore the role of Ca^{2+} in harmonin/cadherin-23 complex formation, CDH23 + exon68 was incubated with glutathione beads, and then incubated with untagged harmonin-a in 50 mM HEPES (pH 7.2), 150 mM KCl, 1 mM Tris(2-carboxyethyl)phosphine (TCEP) at 4°C for 2 h. The concentration of free Ca^{2+} was estimated by Igor Pro software (Wavemetrics, Portland, OR, USA).

Cell culture and immunocytofluorescence analysis

The cDNA constructs encoding full-length harmonin-a and CDH23 + exon68 were cloned into the pEGFP vector, and the construct encoding the PH domain (residues 16–132) of phospholipase C (BC015249) was cloned into the pCMV-Myc vector. For transient transfection experiments, HeLa cells were transfected with the DNA of interest using lipofectamine™ 2000 (Invitrogen), and cells were grown for 24 h before fixation. For PI(4,5)P_2 enrichment at the plasma membrane, cells were incubated with 100 μM H_2O_2 for 20 min before fixation. For immunocytofluorescence experiments, cell samples were fixed using 4% paraformaldehyde (PFA) in phosphate-buffered saline (PBS), stained with a primary antibody for 1 h, washed in PBS three times for 5 min, stained with a secondary antibody for 1 h, washed as above and mounted using Fluorosave (Calbiochem, USA).

Cochlear dissection and immunostaining

Whole-mount preparations of the mouse organ of Corti were obtained as follows. Animals were killed by exposure to CO_2 followed by decapitation, and the inner ears were removed and placed in PBS. The organ of Corti was exposed by removing the stria vascularis, and the tissues were fixed by immersion in 4% PFA in PBS for 1 h. The samples were washed three times in PBS, incubated at room temperature for 1 h in PBS containing 20% goat serum and stained overnight with the primary antibodies diluted in PBS containing 1% BSA. The samples were washed three times in PBS and incubated with either Alexa 488-conjugated or Cy3-conjugated goat anti-rabbit Fab'2 antibodies diluted in PBS containing 20% goat serum, at room temperature for 1 h. After three washes in PBS, the tectorial membrane was carefully removed, and the pieces were mounted using Fluorosave. Samples were analyzed by means of a Zeiss LSM510 Meta confocal microscope.

Lipids and preparation of vesicles

PI, phosphatidylinositol 4-phosphate (PI4P), phosphatidylinositol 5-phosphate (PI5P), PI(4,5)P_2, phosphatidylethanola-

mine (PE), phosphatidylserine (PS), phosphatidylcholine (PC) were purchased from Avanti Polar Lipids (AL, USA). Phospholipids were mixed in the following molar ratios: 35% PC, 13% PS, 35% PE and 17% either PI or PIP. Large unilamellar vesicles (LUVs) were prepared by the rehydration of argon-dried lipids in buffer A (20 mM HEPES pH 7.2, 150 mM KCl, 1 mM TCEP), followed by sonication, filtration on a 0.4 μm pore size filter (Millipore) and extrusion through a 100 nm pore size filter in a mini-extruder (Avanti).

SPR experiments

SPR experiments were performed on a Biacore 2000 system (GE Healthcare), equilibrated at 25°C with buffer A. For cadherin-23/harmonin-a interactions, 300–600 resonance units (RU ≈ pg/mm^2) of GST-fused CDH23 constructs were captured on an anti-GST antibody-coupled CM5 sensorchip surface (GE Healthcare), over which the full-length harmonin-a and its fragments were then flowed at 20 μl/min for 90 s. For harmonin-a/myosin VIIa and cadherin-23/myosin VIIa interactions, harmonin-a (1500 RU) and CDH23 (1700 RU) were covalently immobilized on a CM5 sensorchip, over which the myosin VIIa tail was flowed at 30 μl/min for 120 s. Protein–lipid interactions were monitored using a lipophilic L1 sensorchip (GE Healthcare) on which 7000–8500 RU of the different LUVs were captured, and proteins were then flowed over the LUV at 10 μl/min for 300 s.

SUPPLEMENTARY MATERIAL

Supplementary Material is available at *HMG* online.

ACKNOWLEDGEMENTS

The authors thank Muriel Delepierre for NMR spectra, Raphaël Etournay and Alexandre Chenal for their advice in the preparation of LUV, Beatrice Amigues for myosin VIIa tail preparation, Bruno Baron for circular dichroism experiments, Jacqueline Levilliers for her help in the manuscript preparation and the staff of Dynamic Imaging platform of the Pasteur Institute.

Conflict of Interest statement. None declared.

FUNDING

This work was supported by LHW-Stiftung, Fondation Orange, Conny Maeva Foundation, ANR-05-MRAR-015-01, Raymonde and Guy Strittmatter Foundation (under the aegis of Fondation de France), FAUN Stiftung (Suchert Foundation). Funding to pay the Open Access Charge was provided by Unite de Genetique et Physiologie de l'Audition, Institut Pasteur, France.

REFERENCES

1. Pickles, J.O., von Perger, M., Rouse, G.W. and Brix, J. (1991) The development of links between stereocilia in hair cells of the chick basilar papilla. *Hear. Res.*, **54**, 153–163.
2. Goodyear, R.J., Marcotti, W., Kros, C.J. and Richardson, G.P. (2005) Development and properties of stereociliary link types in hair cells of the mouse cochlea. *J. Comp. Neurol.*, **485**, 75–85.
3. Petit, C. and Richardson, G.P. (2009) Linking genes underlying deafness to hair-bundle development and function. *Nat. Neurosci.*, **12**, 703–710.
4. Lagziel, A., Ahmed, Z.M., Schultz, J.M., Morell, R.J., Belyantseva, I.A. and Friedman, T.B. (2005) Spatiotemporal pattern and isoforms of cadherin 23 in wild type and waltzer mice during inner ear hair cell development. *Dev. Biol.*, **280**, 295–306.
5. Michel, V., Goodyear, R.J., Weil, D., Marcotti, W., Perfettini, I., Wolfrum, U., Kros, C., Richardson, G.P. and Petit, C. (2005) Cadherin 23 is a component of the transient lateral links in the developing hair bundles of cochlear sensory cells. *Dev. Biol.*, **280**, 281–294.
6. Bolz, H., von Brederlow, B., Ramirez, A., Bryda, E.C., Kutsche, K., Nothwang, H.G., Seeliger, M., del, C.S.C.M., Vila, M.C., Molina, O.P. *et al.* (2001) Mutation of CDH23, encoding a new member of the cadherin gene family, causes Usher syndrome type 1D. *Nat. Genet.*, **27**, 108–112.
7. Bork, J.M., Peters, L.M., Riazuddin, S., Bernstein, S.L., Ahmed, Z.M., Ness, S.L., Polomeno, R., Ramesh, A., Schloss, M., Srisailpathy, C.R.S. *et al.* (2001) Usher syndrome 1D and nonsyndromic autosomal recessive deafness DFNB12 are caused by allelic mutations of the novel cadherin-like gene *CDH23*. *Am. J. Hum. Genet.*, **68**, 26–37.
8. Ahmed, Z.M., Riazuddin, S., Bernstein, S.L., Ahmed, Z., Khan, S., Griffith, A.J., Morell, R.J., Friedman, T.B., Riazuddin, S. and Wilcox, E.R. (2001) Mutations of the protocadherin gene *PCDH15* cause Usher syndrome type 1F. *Am. J. Hum. Genet.*, **69**, 25–34.
9. Alagramam, K.N., Yuan, H., Kuehn, M.H., Murcia, C.L., Wayne, S., Srisailpathy, C.R.S., Lowry, R.B., Knaus, R., Van Laer, L., Bernier, F.P. *et al.* (2001) Mutations in the novel protocadherin *PCDH15* cause Usher syndrome type 1F. *Hum. Mol. Genet.*, **10**, 1709–1718.
10. Bitner-Glindzicz, M., Lindley, K.J., Rutland, P., Blaydon, D., Smith, V.V., Milla, P.J., Hussain, K., Furth-Lavi, J., Cosgrove, K.E., Shepherd, R.M. *et al.* (2000) A recessive contiguous gene deletion causing infantile hyperinsulinism, enteropathy and deafness identifies the Usher type 1C gene. *Nat. Genet.*, **26**, 56–60.
11. Verpy, E., Leibovici, M., Zwaenepoel, I., Liu, X.-Z., Gal, A., Salem, N., Mansour, A., Blanchard, S., Kobayashi, I., Keats, B.J.B. *et al.* (2000) A defect in harmonin, a PDZ domain-containing protein expressed in the inner ear sensory hair cells, underlies Usher syndrome type 1C. *Nat. Genet.*, **26**, 51–55.
12. Weil, D., Blanchard, S., Kaplan, J., Guilford, P., Gibson, F., Walsh, J., Mburu, P., Varela, A., Levilliers, J., Weston, M.D. *et al.* (1995) Defective myosin VIIA gene responsible for Usher syndrome type 1B. *Nature*, **374**, 60–61.
13. Weil, D., El-Amraoui, A., Masmoudi, S., Mustapha, M., Kikkawa, Y., Lainé, S., Delmaghani, S., Adato, A., Nadifi, S., BenZina, Z. *et al.* (2003) Usher syndrome type I G (USH1G) is caused by mutations in the gene encoding SANS, a protein that associates with the USH1C protein, harmonin. *Hum. Mol. Genet.*, **12**, 463–471.
14. Lefèvre, G.M., Michel, V., Weil, D., Lepelletier, L., Bizard, E., Wolfrum, U., Hardelin, J.-P. and Petit, C. (2008) A core cochlear phenotype in USH1 mouse mutants implicates fibrous links of the hair bundle in its cohesion, orientation and differential growth. *Development*, **135**, 1427–1437.
15. Boëda, B., El-Amraoui, A., Bahloul, A., Goodyear, R., Daviet, L., Blanchard, S., Perfettini, I., Fath, K.R., Shorte, S., Reiners, J. *et al.* (2002) Myosin VIIa, harmonin, and cadherin 23, three Usher I gene products, cooperate to shape the sensory hair cell bundle. *EMBO J.*, **21**, 6689–6699.
16. Senften, M., Schwander, M., Kazmierczak, P., Lillo, C., Shin, J.B., Hasson, T., Geleoc, G.S., Gillespie, P.G., Williams, D., Holt, J.R. *et al.* (2006) Physical and functional interaction between protocadherin 15 and myosin VIIa in mechanosensory hair cells. *J. Neurosci.*, **26**, 2060–2071.
17. Siemens, J., Kazmierczak, P., Reynolds, A., Sticker, M., Littlewood-Evans, A. and Muller, U. (2002) The Usher syndrome proteins cadherin 23 and harmonin form a complex by means of PDZ-domain interactions. *Proc. Natl Acad. Sci. USA*, **99**, 14946–14951.
18. Adato, A., Kikkawa, Y., Reiners, J., Alagramam, K.N., Weil, D., Yonekawa, H., Wolfrum, U., El-Amraoui, A. and Petit, C. (2005) Interactions in the network of Usher syndrome type 1 proteins. *Hum. Mol. Genet.*, **14**, 347–356.
19. Pan, L., Yan, J., Wu, L. and Zhang, M. (2009) Assembling stable hair cell tip link complex via multidentate interactions between harmonin and cadherin 23. *Proc. Natl Acad. Sci. USA*, **106**, 5575–5580.

20. Ahmed, Z.M., Goodyear, R., Riazuddin, S., Lagziel, A., Legan, P.K., Behra, M., Burgess, S.M., Lilley, K.S., Wilcox, E.R., Riazuddin, S. *et al.* (2006) The tip-link antigen, a protein associated with the transduction complex of sensory hair cells, is protocadherin-15. *J. Neurosci.*, **26**, 7022–7034.
21. Kazmierczak, P., Sakaguchi, H., Tokita, J., Wilson-Kubalek, E.M., Milligan, R.A., Muller, U. and Kachar, B. (2007) Cadherin 23 and protocadherin 15 interact to form tip-link filaments in sensory hair cells. *Nature*, **449**, 87–91.
22. Pickles, J.O., Comis, S.D. and Osborne, M.P. (1984) Cross-links between stereocilia in the guinea pig organ of Corti, and their possible relation to sensory transduction. *Hear. Res.*, **15**, 103–112.
23. Grillet, N., Xiong, W., Reynolds, A., Kazmierczak, P., Sato, T., Lillo, C., Dumont, R.A., Hintermann, E., Sczaniecka, A., Schwander, M. *et al.* (2009) Harmonin mutations cause mechanotransduction defects in cochlear hair cells. *Neuron*, **62**, 375–387.
24. Michalski, N., Michel, V., Caberlotto, E., Lefèvre, G.M., van Aken, A.F.J., Tinevez, J.-Y., Bizard, E., Houbron, C., Weil, D., Hardelin, J.-P. *et al.* (2009) Harmonin-b, an actin-binding scaffold protein, is involved in the adaptation of mechanoelectrical transduction by sensory hair cells. *Pflügers Arch.*, **459**, 115–130.
25. Leibovici, M., Safieddine, S. and Petit, C. (2008) Mouse models of human hereditary deafness. *Curr. Top. Dev. Biol.*, **84**, 385–429.
26. Jemth, P. and Gianni, S. (2007) PDZ domains: folding and binding. *Biochemistry*, **46**, 8701–8708.
27. Beurg, M., Fettiplace, R., Nam, J.H. and Ricci, A.J. (2009) Localization of inner hair cell mechanotransducer channels using high-speed calcium imaging. *Nat. Neurosci.*, **12**, 553–558.
28. Yan, J., Pan, L., Chen, X., Wu, L. and Zhang, M. (2010) The structure of the harmonin/sans complex reveals an unexpected interaction mode of the two Usher syndrome proteins. *Proc. Natl Acad. Sci. USA*, **107**, 4040–4045.
29. Kros, C.J., Marcotti, W., van Netten, S.M., Self, T.J., Libby, R.T., Brown, S.D., Richardson, G.P. and Steel, K.P. (2002) Reduced climbing and increased slipping adaptation in cochlear hair cells of mice with Myo7a mutations. *Nat. Neurosci.*, **5**, 41–47.
30. Gillespie, P.G. and Müller, U. (2009) Mechanotransduction by hair cells: models, molecules, and mechanisms. *Cell*, **139**, 33–44.
31. Inoue, A. and Ikebe, M. (2003) Characterization of the motor activity of mammalian myosin VIIA. *J. Biol. Chem.*, **278**, 5478–5487.
32. Henn, A. and De La Cruz, E. (2005) Vertebrate myosin VIIb is a high duty ratio motor adaptedfor generating and maintaining tension. *J. Biol. Chem.*, **280**, 39665–39676.
33. El-Amraoui, A., Bahloul, A. and Petit, C. (2008) Myosin VII. InColuccio, L.M. (ed.), *Myosins: A Superfamily of Molecular Motors*. Springer, New York, **Vol. 7**, pp. 353–373.
34. Hirono, M., Denis, C.S., Richardson, G.P. and Gillespie, P.G. (2004) Hair cells require phosphatidylinositol 4,5-bisphosphate for mechanical transduction and adaptation. *Neuron*, **44**, 309–320.
35. Gallardo, R., Ivarsson, Y., Schymkowitz, J., Rousseau, F. and Zimmermann, P. (2010) Structural diversity of PDZ-lipid interactions. *Chembiochemistry*, **11**, 456–467.
36. Varnai, P. and Balla, T. (1998) Visualization of phosphoinositides that bind pleckstrin homology domains: calcium- and agonist-induced dynamic changes and relationship to myo-[3H]inositol-labeled phosphoinositide pools. *J. Cell Biol.*, **143**, 501–510.
37. Shasby, D.M., Winter, M. and Shasby, S.S. (1988) Oxidants and conductance of cultured epithelial cell monolayers: inositol phospholipid hydrolysis. *Am. J. Physiol.*, **255**, C781–C788.
38. El-Amraoui, A., Sahly, I., Picaud, S., Sahel, J., Abitbol, M. and Petit, C. (1996) Human Usher IB/mouse *shaker-1*; the retinal phenotype discrepancy explained by the presence/absence of myosin VIIA in the photoreceptor cells. *Hum. Mol. Genet.*, **5**, 1171–1178.